Distribution and Transmission Coordinated Dispatch Under Joint Electricity and Carbon Day-Ahead Markets

Wandry Rodrigues Faria[a], Gregorio Muñoz-Delgado[b], Javier Contreras[b] and Benvindo Rodrigues Pereira Jr.[a]

[a]Department of Electrical Engineering and Computation, University of São Paulo, São Carlos – SP, Brazil
[b]Escuela Técnica Superior de Ingeniería Industrial, Universidad de Castilla-La Mancha, 13071 Ciudad Real, Spain

ARTICLE INFO

Keywords:
Bilevel programming
Distribution system operation
Joint electricity and carbon trading
Wholesale day-ahead markets

Abstract

Worldwide efforts to attain a more renewable-based energy matrix have led to the creation of carbon emission-related markets. Simultaneously, the increasing penetration, mostly of renewable-based sources, in distribution networks may allow distribution system operators (DSOs) to change their traditional participation in wholesale markets as passive buyers. Over the last few years, many authors have investigated and proposed optimization models for the strategic participation of DSOs in electricity markets. Nonetheless, proposals regarding the DSO as a strategic agent in both electricity and carbon-related markets are rare. In this paper, we propose a stochastic bilevel formulation to address this gap. The economic and operational constraints of each stakeholder are considered in the model. Additionally, the problem is written in a convex formulation for which finite convergence to optimality is guaranteed. The formulation was tested for a 14-node transmission system and a 34-node distribution system in which dispatchable and non-dispatchable energy sources, energy storage systems, and demand response units are installed. The results show the DSO's capacity to place strategic bids in both market environments to maximize its profit, which features intentionally taking financial losses in the carbon allowance market to maximize the overall profit due to the income maximization in the electricity market. Finally, an additional case study with a 123-node distribution system shows the proposed method's scalability.

1. Introduction

1.1. Background and Literature Review

Environmental efforts over the last four decades have led many countries to agree to gradual reductions in carbon emissions [1, 2]. The electricity sector was responsible for 65% of the total greenhouse gas emissions in the European Union in 2018 [3]. Even though the portion of emissions due to electricity generation has reduced over the last few years, reaching approximately 49% in 2022, the sector is still one of the main sources of emissions in the European Union [4]. Given the context of well-established wholesale markets for electricity procurement [5], the development of carbon-related markets to accommodate the demand for less carbon-intense electricity production was expected. In this sense, an efficient way to dissuade greenhouse gas emissions is the employment of the cap-and-trade scheme, which has been adopted in the United States [6] and European Union (EU) [7]. In this framework, each participant in the electricity market is allowed to emit a certain amount of greenhouse gases to produce electricity. Once the participant reaches the allowance limit they can either stop injecting power into the system or buy additional carbon allowances in a market environment [7, 8].

The design of a market for carbon allowances under a cap-and-trade scheme must address the peculiarities of the local energy mix; thus, there may be differences in the regulations of carbon markets for each country. Considering the reality of the cap-and-trade environment of the EU, electricity/heat production, aviation, and energy-intensive industry sectors are covered by the European Union emission trading system (EU ETS) [7]. Each agent of these sectors receives for free an annual amount of carbon allowances, which decreases every year to inhibit greenhouse gas emissions. Additionally, a limited number of carbon allowances are auctioned by the EU ETS and the revenue is used to foment low-carbon innovation and energy transition. Finally, the agents that participate in the EU ETS are allowed to trade carbon allowances amongst themselves, which is possible only if some agents do not use all of their allowances and work as an incentive in the mid- and long-term for investments in reducing their carbon emissions. If an agent fails to comply with their carbon emission limit, heavy fines (that are increasing in value yearly) are imposed as a means to force the agents to avoid such scenario.

Since the electricity production sector is within the scope of the carbon trading system, the adoption of the cap-and-trade strategy to limit and gradually reduce greenhouse gas emissions affects the economic dispatch problem since producing electricity with cheap but highly carbon-intense generators may either become infeasible or lead to additional expenses in the carbon market. In this sense, many authors have proposed new approaches to the optimal power flow (OPF) problem considering carbon emissions, the so-called carbon-aware OPF. The proposals developed in this field can be categorized into two strands. The first, addressed in this paragraph, encompasses centralized formulations, i.e.,

wandry@usp.br (W.R. Faria); gregorio.munoz@uclm.es (G. Muñoz-Delgado); javier.contreras@uclm.es (J. Contreras); brpjunior@usp.br (B.R. Pereira Jr.)
ORCID(s): 0000-0002-8757-7595 (W.R. Faria); 0000-0003-0300-1183 (G. Muñoz-Delgado); 0000-0002-9395-3964 (J. Contreras); 0000-0003-2157-5148 (B.R. Pereira Jr.)

Nomenclature

Indices

b	Index for bid block.
g	Index for generators.
i, j	Index for nodes.
ij, ki	Index for distribution lines.
l	Index for transmission lines.
s	Index for scenarios.
t	Index for time periods.

Sets

$\mathcal{B}_g$	Set of bids provided by generator g.
$\mathcal{G}_D$	Set of distribution-connected generators.
$\mathcal{G}_i$	Set of generators connected to node i.
$\mathcal{G}_T$	Set of transmission-connected generators.
$\mathcal{L}_D$	Set of distribution lines.
$\mathcal{L}_T$	Set of transmission lines.
N_D	Set of distribution nodes.
N_T	Set of transmission nodes.
N_∞	Set of interface nodes.
S	Set of scenarios.
T	Set of time periods.

Parameters

$A_{i,l}$	Element of the incidence matrix, which is equal to 1 if node i is the sending node of transmission line l, -1 if node i is the receiving node and 0 otherwise.
$C^D_{g,b}, C^T_{g,b}$	Distribution and transmission-connected generators' bids.
H	Number of time periods.
$\overline{I}_{ij}$	Capacity of distribution lines.
$\mathcal{K}^L_i$	Relationship between active and reactive power, i.e., $\tan(\arccos(\text{power factor}))$.
$\mathcal{K}^r_{g,t,s}$	Renewable-based power availability.
$L^D_{i,t,s}$	Power demand of a distribution node.
$L^T_{i,t,s}$	Power demand of a transmission node.
$p_{s,t}$	Weight of scenario s at period t.
$\overline{S}^D_g, \overline{P}^T_g$	Maximum power injection of generators.
$\mathcal{P}_g$	Type of generator g (conventional $\mathcal{P}_C$ or renewable $\mathcal{P}_R$).
$\overline{P}^D_{g,b}, \overline{P}^T_{g,b}$	Size of the generator's electricity block bid.
$\underline{P}^{ESS}_i, \overline{P}^{ESS}_i$	Maximum charging and discharging power of storage systems.
$\underline{P}^{LS}_i, \overline{P}^{LS}_i$	Maximum nodal load increase/reduction.
$\overline{P}^{SE}_i$	Distribution substation capacity.
$\overline{PF}_l$	Power flow capacity of transmission lines.
R_{ij}	Resistance of distribution lines.
$\underline{SOC}^{ESS}_i, \overline{SOC}^{ESS}_i$	Maximum and minimum state of charge of the storage systems.
$SOC^{(0)}_i$	Initial state of charge of the storage systems.
U	Rigidity of the carbon emission regulation.
$\overline{V}_i, \underline{V}_i$	Maximum and minimum nodal voltage.
X_l	Reactance of transmission lines.
X_{ij}	Reactance of distribution lines.
Λ	Average carbon intensity of the entire power system.
γ^D_g, γ^T_g	Generator's carbon intensity.
$\overline{\Gamma}^D_t, \overline{\Gamma}^T_t$	Distribution and transmission system carbon emission allowance per time period.

Distribution Side Decision Variables

$I^{SQ}_{ij,t,s}$	Distribution line current magnitude squared.
$P^D_{g,t,s}, Q^D_{g,t,s}$	Generator active and reactive power dispatch.
$P_{ij,t,s}, Q_{ij,t,s}$	Active and reactive power flow on distribution lines.
$P^{ESS}_{i,t,s}$	Power charge/discharge of storage systems.
$P^{LS}_{i,t,s}$	Nodal load shift.
$V^{SQ}_{i,t,s}$	Nodal voltage magnitude squared.
$SOC_{i,t,s}$	State of charge of energy storage systems.
$\nu^D_{g,t,s}$	Generator's carbon emission.
$\pi^C_{t,s}, \pi^E_{i,t,s}$	Bids on the carbon and electricity markets.
$\rho^D_{g,b,t,s}$	Accepted bid of block b.
$\varrho^D_{g,t,s}$	Carbon allowances absorbed/provided by generator g.

Transmission Side Decision Variables

$P^T_{g,t,s}$	Generator's total power dispatch.
$PF_{l,t,s}$	Power flow on transmission lines.
$P^{SE}_{i,t,s}, Q^{SE}_{i,t,s}, \varrho^{SE}_{t,s}$	Active and reactive power and carbon allowance trades in the wholesale market.
$\delta_{i,t,s}$	Voltage angle of transmission nodes.
$\nu^T_{g,t,s}$	Generator's carbon emission.
$\rho^T_{g,b,t,s}$	Accepted bid of block b.
$\varrho^T_{g,t,s}$	Carbon allowances absorbed/provided by generator g.

there is a single entity responsible for dispatching the assets based on input data. The authors of [9] propose the use of demand response (DR) and energy storage system (ESS) associated with a new method to trace nodal carbon emission costs as a means to attain the transmission system's low-carbon optimal operation. In [10], the authors develop an optimal energy flow model considering the combination of electricity, natural gas, and heat systems. The authors determine the local marginal prices (LMPs) and investigate the impacts of carbon emission on these values. The integration of electrical and thermal systems via the employment of heat pumps and electric boiler-heat storage devices is investigated

in [11]. The proposed model manages renewable intermittent and dispatchable power sources, as well as storage units, to minimize wind spillage and greenhouse gas emissions. The multi-objective model presented in [12] considers the operation of DR, coal power plants equipped with carbon capture and ESSs to simultaneously minimize carbon emissions and generation costs. It should be highlighted that in [9] and [12], the electricity prices are parameters to which the distributed energy resource (DER) owner can simply react, while in [10] and [11] the bids/offers are parameters which the market operator can accept or not. Thus, for each of these proposals, there is always only one decision-maker.

The second strand of approaches focuses on modeling the market environments and performing the market clearing process, which calls for modeling multiple stakeholders. The authors of [13] propose a two-layered peer-to-peer (P2P) market. The prosumers trade energy and carbon allowances (E&C) directly among themselves in the first layer. The unmet demands/offers are aggregated by the microgrid operator (MGO) and traded among other MGOs in another market environment modeled as the second layer. A blockchain structure is proposed to guarantee the trades between agents at a low computational cost. However, there is no regard for the power system's physical limits. The proposal presented in [14] considers the distribution system operator (DSO) as a mediator through which MGOs trade E&C. The authors consider the existence of a coalition of MGOs whose profit is maximized by the optimal asset management provided by the DSO. Next, the authors propose a method to optimally distribute the revenue among the individual MGOs. Another distribution-level market environment for trading E&C is proposed in [15]. The authors consider the following entities: the DSO, responsible for providing E&C price incentives based on a carbon-aware OPF, and the prosumers connected to the distribution system (DS) who trade power and carbon allowances amongst themselves in a P2P market structure.

It should be stressed that the DSO is able to trade E&C with the transmission system via some kind of wholesale environment in approaches [14] and [15]. Nonetheless, the DSO is modeled as a price-taker in this environment, i.e., the wholesale E&C prices are constant regardless of the DSO's actions. Additionally, the transmission system's physical constraints are disregarded. In this sense, other authors focus on modeling the wholesale market while considering the effects of the participation of DSOs in the clearing prices. References [16] and [17] present a two-stage model for the clearing process of an E&C wholesale market. The first stage regards the operational limits of the transmission system and its assets and provides E&C prices for the second stage problem in which flexible consumers react to such prices. The two problems are solved iteratively until the prices and demands cease to change. It is fundamental to point out that the consumers are modeled as aggregated PQ loads managed by electricity retailers. Thus, an agent as flexible as an active DS, capable of both demanding and supplying E&C, is not regarded. A resembling approach is proposed in [18], wherein the authors formulate a carbon-constrained hierarchical power dispatch for a multi-energy problem composed of electricity and gas systems. Similarly to [16] and [17], the marginal prices are determined by solving a carbon-aware OPF, and the reaction of flexible consumers is formulated as a second problem. The authors of [18] combine mathematical programming and a swarm-based metaheuristic to solve the entire problem. Another multi-energy problem is investigated in [19], wherein a multi-level formulation is proposed. The authors consider the E&C price calculation as the upper-level problem, which is the result of OPF and carbon emission flow routines. The optimal reaction of distribution-level multi-energy systems is modeled at the lower level. Given that the E&C prices are given by dual variables, solving the bilevel programming (BLP) model by writing its mathematical program with equilibrium constraints (MPEC) form is not possible, as the price variables would not be accessible. Thus, the authors chose to solve the problem iteratively, employing a bisection-based method to ensure convergence. Nonetheless, it is important to stress that this method cannot attest to the solution's optimality.

1.2. Motivation and Contributions

Although the participation of DSs is considered in the approaches mentioned in the previous subsection, their line and nodal constraints are not taken into account in any of the approaches. Furthermore, the agent equivalent to a DSO is regarded as a non-strategic price-maker of the wholesale market in all of the approaches. The formulation of DSOs as strategic-price makers in electricity-only wholesale markets is not rare [20–22]; nonetheless, few analogous models in which the E&C environments are formulated can be found. These characteristics can be found in [23] wherein a BLP formulation is proposed to model the DSO's participation in the E&C wholesale market as a strategic-price maker. However, at least three short-comings of this proposal should be highlighted 1) the renewable-based sources, as well as uncertainties associated with such power sources and the hourly demands, are not considered; 2) the DS constraints disregard reactive power; and 3) the problem is solved as a nonlinear programming (NLP) instance for which convergence to the optimal solution is not guaranteed.

In this context, we propose a BLP approach designed to provide the DSO with strategics when participating in the E&C day-ahead wholesale markets to address the mentioned gaps. The stakeholders modeled in the optimization problem are the DSO and the independent system operator (ISO), who is considered to manage both the transmission system and the E&C markets, similarly to [22]. Each stakeholder is responsible for the safe operation of their assets; in this sense, the operational limits of transmission and distribution systems are considered, which are totally or partially disregarded in the approaches presented in [14–18]. In accordance to reference [23], which is the most similar proposal found in the literature, in the formulation presented in this paper, the DSO and the ISO are capable of both selling and buying

Table 1
Comparison Between the Proposed Approach and the State-of-the-Art Approaches Jointly Addressing E&C Markets

Ref.	DSO Price-Maker in Wholesale Environment	Power System Model				Solving Technique	
		T.S.C.	D.S.C.	R.P.F	Uncertainty	BLP-based	Optimality Guarantee
[13]	✗	✗	✗	✗	✗	✗	✗
[14]	✗	✗	✓	✓	✗	✓	✓
[15]	✗	✗	✓	✓	✗	✗	✗
[16–19]	✓	✓	✗	✗	✗	✓	✗
[23]	✓	✓	✓	✗	✗	✓	✗
This paper	✓	✓	✓	✓	✓	✓	✓

T.S.C. - Transmission system network constraints; D.S.C. - Distribution system network constraints; R.P.F - Reactive power flow; LDM - Local distribution market; WM - Wholesale market.

E&C. Additionally, DR, namely load shift, and ESSs are considered in the DS. However, in this paper, conventional- and renewable-based power plants are installed in the transmission and distribution systems, which calls for uncertainty consideration in both power systems, a feature that is not within the scope of the work presented in [23]. The resulting BLP model is transformed into a MPEC formulation, which is then converted into a mixed-integer quadratically constrained programming (MIQCP). A comparison between the proposed formulation and other similar approaches published in the specific literature is presented in Table 1. In this sense, the main contributions of this manuscript consist of the combination of the following topics:

1. Expanding the existing consideration of the DSO as a strategic-price maker agent of the wholesale electricity market [20–22] to the E&C market environments;
2. Simultaneously considering the network constraints of the transmission and distribution systems in the market-clearing process, which is disregarded in references [13–19];
3. Addressing the uncertainties related to renewable-based power injection and short-time load variation in both transmission and distribution systems via stochastic programming, which is not included in [13–19] and [23];
4. Reformulation of the MPEC problem, which is originally a NLP model, as a MIQCP. In this sense, although the original MPEC formulation guarantees the equilibrium between the agents' objectives, given its nonlinear nonconvex nature, the solution may converge to local optima. Unlinke the formulations proposed in [13, 15–19] and [23], the proposed MIQCP ensures finite convergence to the optimal DSO bidding.

1.3. Paper Structure

In addition to this introductory section, the paper is structured as follows. The optimization problem's mathematical formulation is presented in Section 2. In Section 3, we validate the proposed method and present numerical results. Finally, the conclusions are drawn in Section 4. Additionally, the input data and the complete mathematical manipulation to attain the proposed MIQCP formulation are available in an electronic companion [24].

2. Problem Formulation

In this paper, we propose the bilevel model illustrated in Fig. 1 to represent the interaction between the DSO and the ISO in the E&C wholesale markets. The DSO is considered to be the upper-level agent, who is responsible for submitting optimal bids/offers to the E&C wholesale markets. On the other hand, the ISO, whose attribution is to conduct the clearing process of the E&C markets, reacts to the DSO's bids/offers by determining how much power/carbon allowances will be traded. Henceforth, we will refer to the clearing processes, which define the E&C trades, simply as ISO.

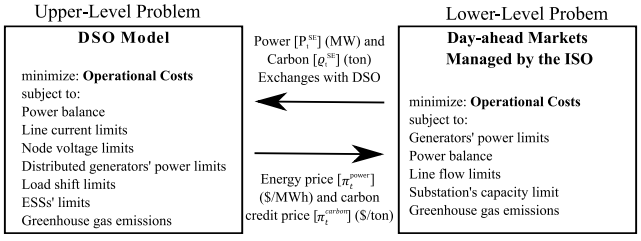

Figure 1: Bilevel model illustration

The electricity and carbon markets are designed to be two independent environments, as proposed in [15]. However, the rewarding method differs from that employed in [15] given the bilevel model proposed in this paper. In this approach, both markets adopt the LMP as the rewarding method. The LMP of a market product is given by the dual variable of its balance equation (λ for electricity and ψ for carbon allowances) [22, 25]. The following assumptions were made to develop the formulation proposed in this paper.

1. There are at least two wholesale market environments, namely an electricity market and a carbon allowance market, where agents can freely offer and purchase the corresponding energy product;
2. The DSOs are allowed to participate in the wholesale markets offering and purchasing any amount of

electricity and carbon allowances like any other participant of these markets. On the other hand, the owners of DERs cannot participate in the wholesale markets. This hypothesis has been vented for electricity wholesale markets as a means to minimize the number of agents participating in the market and grant the DSO some control over the decisions of the owners of DERs as their power injections depend on the DS grid availability [20–22, 26];

3. The DSOs are not usually the owners of DERs and, therefore, cannot control their power injections. However, we assume that there is an additional distribution-level market, which is not within the scope of this paper, managed and cleared by the DSO. Once the distribution market is cleared, the DSO is able to operate as an aggregator of the DERs, or as a retailer, in the wholesale market. Similar assumptions have been made by other works that focused on the DSO participation in wholesale electricity markets [27–30].

Thus, assuming these hypotheses, the optimization problem can be formulated as follows.

2.1. DSO Optimization Model - Upper-Level Problem

The proposed formulation for the DSOs in the upper-level optimization problem is as follows:

$$\min \sum_{s\in\mathcal{S}}\sum_{t\in\mathcal{T}} p_{s,t}\left[\sum_{g\in\mathcal{G}_D}\sum_{b\in\mathcal{B}_g}\left(C^D_{g,b}\rho^D_{g,b,t,s}\right) + \psi_{t,s}\varrho^{SE}_{t,s} + \sum_{i\in\mathcal{N}_\infty}\lambda_{i,t,s}P^{SE}_{i,t,s}\right] \tag{1}$$

subject to:

$$\sum_{g\in\mathcal{G}_i} P^D_{g,t,s} + \sum_{ki\in\mathcal{L}_D} P_{ki,t,s} - \sum_{ij\in\mathcal{L}_D}\left(P_{ij,t,s} + R_{ij}I^{SQ}_{ij,t,s}\right) + P^{ESS}_{i,t,s} = P^{LS}_{i,t,s} + L^D_{i,t,s} \quad \forall i\in\mathcal{N}_D, t\in\mathcal{T}, s\in\mathcal{S} \tag{2}$$

$$\sum_{g\in\mathcal{G}_i} P^D_{g,t,s} + \sum_{ki\in\mathcal{L}_D} P_{ki,t,s} - \sum_{ij\in\mathcal{L}_D}\left(P_{ij,t,s} + R_{ij}I^{SQ}_{ij,t,s}\right) + P^{SE}_{i,t,s} + P^{ESS}_{i,t,s} = P^{LS}_{i,t,s} + L^D_{i,t,s} \quad \forall i\in\mathcal{N}_\infty, t\in\mathcal{T}, s\in\mathcal{S} \tag{3}$$

$$\sum_{g\in\mathcal{G}_i} Q^D_{g,t,s} + \sum_{ki\in\mathcal{L}_D} Q_{ki,t,s} - \sum_{ij\in\mathcal{L}_D}\left(Q_{ij,t,s} + X_{ij}I^{SQ}_{ij,t,s}\right) = \mathcal{K}^L_i\left(P^{LS}_{i,t,s} + L^D_{i,t,s}\right) \quad \forall i\in\mathcal{N}_D, t\in\mathcal{T}, s\in\mathcal{S} \tag{4}$$

$$\sum_{g\in\mathcal{G}_i} Q^D_{g,t,s} + \sum_{ki\in\mathcal{L}_D} Q_{ki,t,s} - \sum_{ij\in\mathcal{L}_D}\left(Q_{ij,t,s} + X_{ij}I^{SQ}_{ij,t,s}\right) + Q^{SE}_{i,t,s} = \mathcal{K}^L_i\left(P^{LS}_{i,t,s} + L^D_{i,t,s}\right) \quad \forall i\in\mathcal{N}_\infty, t\in\mathcal{T}, s\in\mathcal{S} \tag{5}$$

$$V^{SQ}_{i,t,s} - V^{SQ}_{j,t,s} = 2(P_{ij,t,s}R_{ij} + Q_{ij,t,s}X_{ij}) + \left(R^2_{ij} + X^2_{ij}\right)I^{SQ}_{ij,t,s} \quad \forall ij\in\mathcal{L}_D, t\in\mathcal{T}, s\in\mathcal{S} \tag{6}$$

$$P^2_{ij,t,s} + Q^2_{ij,t,s} \le I^{SQ}_{ij,t,s}V^{SQ}_{j,t,s} \quad \forall ij\in\mathcal{L}_D, t\in\mathcal{T}, s\in\mathcal{S} \tag{7}$$

$$0 \le I^{SQ}_{ij,t,s} \le \overline{I}^2_{ij} \quad \forall ij\in\mathcal{L}_D, t\in\mathcal{T}, s\in\mathcal{S} \tag{8}$$

$$\underline{V}^2_i \le V^{SQ}_{i,t,s} \le \overline{V}^2_i \quad \forall i\in\mathcal{N}_D, t\in\mathcal{T}, s\in\mathcal{S} \tag{9}$$

$$(P^D_{g,t,s})^2 + (Q^D_{g,t,s})^2 \le (\overline{S}^D_g)^2 \quad \forall g\in\{\mathcal{G}_D|\mathcal{P}_g = \mathcal{P}_C\}, t\in\mathcal{T}, s\in\mathcal{S} \tag{10}$$

$$(P^D_{g,t,s})^2 + (Q^D_{g,t,s})^2 \le \mathcal{K}^R_{g,t,s}(\overline{S}^D_g)^2 \quad \forall g\in\{\mathcal{G}_D|\mathcal{P}_g = \mathcal{P}_R\}, t\in\mathcal{T}, s\in\mathcal{S} \tag{11}$$

$$\sum_{b\in\mathcal{B}_g}\rho^D_{g,b,t,s} = P^D_{g,t,s} \quad \forall g\in\mathcal{G}_D, t\in\mathcal{T}, s\in\mathcal{S} \tag{12}$$

$$\rho^D_{g,b,t,s} \le \overline{P}^D_{g,b} \quad \forall g\in\mathcal{G}_D, b\in\mathcal{B}_g, t\in\mathcal{T}, s\in\mathcal{S} \tag{13}$$

$$\underline{P}^{LS}_i \le P^{LS}_{i,t,s} \le \overline{P}^{LS}_i \quad \forall i\in\mathcal{N}_D, t\in\mathcal{T}, s\in\mathcal{S} \tag{14}$$

$$\sum_{t\in\mathcal{T}} P^{LS}_{i,t,s} = 0 \quad \forall i\in\mathcal{N}_D, s\in\mathcal{S} \tag{15}$$

$$\underline{P}^{ESS}_i \le P^{ESS}_{i,t,s} \le \overline{P}^{ESS}_i \quad \forall i\in\mathcal{N}_D, t\in\mathcal{T}, s\in\mathcal{S} \tag{16}$$

$$\underline{SOC}_i \le SOC_{i,t,s} \le \overline{SOC}_i \quad \forall i\in\mathcal{N}_D, t\in\mathcal{T}, s\in\mathcal{S} \tag{17}$$

$$SOC_{i,1} = SOC^{(0)}_i - P^{ESS}_{i,1,s} \quad \forall i\in\mathcal{N}_D, s\in\mathcal{S} \tag{18}$$

$$SOC_{i,t,s} = SOC_{i,t-1,s} - P^{ESS}_{i,t,s} \quad \forall i\in\mathcal{N}_D, t = 2...H, s\in\mathcal{S} \tag{19}$$

$$SOC^{(0)}_i = SOC_{i,H,s} \quad \forall i\in\mathcal{N}_D, s\in\mathcal{S} \tag{20}$$

$$\nu^D_{g,t,s} = \gamma^D_g P^D_{g,t,s} \quad \forall g\in\mathcal{G}_D, t\in\mathcal{T}, s\in\mathcal{S} \tag{21}$$

$$\sum_{g\in\mathcal{G}_D}\varrho^D_{g,t,s} = -\varrho^{SE}_{t,s} \quad \forall t\in\mathcal{T}, s\in\mathcal{S} \tag{22}$$

$$\sum_{g\in\mathcal{G}_D}\left(\nu^D_{g,t,s} + \varrho^D_{g,t,s}\right) \le \overline{\Gamma}^D_t \quad \forall t\in\mathcal{T}, s\in\mathcal{S} \tag{23}$$

The DSO optimization problem is designed to minimize the DS's operational costs. The first term of (44) addresses the generation costs of units connected to the DS. The DSO's revenues from electricity and carbon markets are given by the second and third terms of (44), respectively. Constraints (2)–(5) guarantee the DS's active and reactive power balance. The second-order conic programming-based power flow equations are described in (6)–(7). Constraints (8)–(9) ensure that the currents and voltages are kept within pre-defined ranges. The limits for conventional- and renewable-based generators power injection are modeled in (10)–(11), while the DR limits are considered in (14). Equation (15) ensures that the electricity consumed by each load is the same with or without load shifting. The limits for the ESSs' charge/discharge and state of charge (SOC), respectively, are imposed in (16)–(17). The ESS's SOC is calculated in (18)–(19). Constraint (20) guarantees that each ESS's SOC at the end of the planning horizon is the same as its initial value. The carbon emission due to conventional-based generators producing active power is calculated in (21). The carbon balance, which indicates the sources of the carbon allowances traded between DSO and ISO, is shown in (22). Finally, the DS's carbon allowance limit per time

period is enforced in (23) [15]. It should be mentioned that $\lambda_{i,t,s}$ and ψ_t are, respectively, the electricity and carbon allowance shadow prices, which are dual variables of the lower-level problem.

2.2. ISO Optimization Model - Lower-Level Problem

The lower-level problem is formulated as follows:

$$\min \sum_{s\in\mathcal{S}}\sum_{t\in\mathcal{T}} p_{s,t}\left[\sum_{g\in\mathcal{G}_T}\sum_{b\in\mathcal{B}_g}\left(C^T_{g,b}\rho^T_{g,b,t,s}\right) - \pi^E_{t,s}P^{SE}_{i,t,s} - \pi^C_{t,s}\varrho^{SE}_{t,s}\right] \tag{24}$$

subject to:

$$\sum_{g\in\mathcal{G}_i} P^T_{g,t,s} - \sum_{l\in\mathcal{L}_T} A_{i,l}PF_{l,t,s} = L^T_{i,t,s} \quad \forall i\in\mathcal{N}_T, t\in\mathcal{T}, s\in\mathcal{S} \tag{25}$$

$$\sum_{g\in\mathcal{G}_i} P^T_{g,t,s} - \sum_{l\in\mathcal{L}_T} A_{i,l}PF_{l,t,s} - P^{SE}_{t,s} = L^T_{i,t,s} \quad \forall i\in\mathcal{N}_\infty, t\in\mathcal{T}, s\in\mathcal{S} \tag{26}$$

$$PF_{l,t,s} = \frac{1}{X_l}\sum_{i\in\mathcal{N}_T\cup\mathcal{N}_\infty} A_{i,l}\delta_{i,t,s} \quad \forall l\in\mathcal{L}_T, t\in\mathcal{T}, s\in\mathcal{S} \tag{27}$$

$$0 \le P^T_{g,t,s} \le \overline{P}^T_g \quad \forall g\in\{\mathcal{G}_T|\mathcal{P}_g=\mathcal{P}_C\}, t\in\mathcal{T}, s\in\mathcal{S} \tag{28}$$

$$0 \le P^T_{g,t,s} \le \mathcal{K}^R_{g,t,s}\overline{P}^T_g \quad \forall g\in\{\mathcal{G}_T|\mathcal{P}_g=\mathcal{P}_R\}, t\in\mathcal{T}, s\in\mathcal{S} \tag{29}$$

$$\sum_{b\in\mathcal{B}_g}\rho^T_{g,b,t,s} = P^T_{g,t,s} \quad \forall g\in\mathcal{G}_T, t\in\mathcal{T}, s\in\mathcal{S} \tag{30}$$

$$\rho^T_{g,b,t,s} \le \overline{P}^T_{g,b} \quad \forall g\in\mathcal{G}_T, b\in\mathcal{B}_g, t\in\mathcal{T}, s\in\mathcal{S} \tag{31}$$

$$-\overline{PF_l} \le PF_{l,t,s} \le \overline{PF_l} \quad \forall l\in\mathcal{L}_T, t\in\mathcal{T}, s\in\mathcal{S} \tag{32}$$

$$-\overline{P}^{SE}_i \le P^{SE}_{i,t,s} \le \overline{P}^{SE}_i \quad \forall i\in\mathcal{N}_\infty, t\in\mathcal{T}, s\in\mathcal{S} \tag{33}$$

$$\nu^T_{g,t,s} = \gamma^T_g P^T_{g,t,s} \quad \forall g\in\mathcal{G}_T, t\in\mathcal{T}, s\in\mathcal{S} \tag{34}$$

$$\sum_{g\in\mathcal{G}_T}\varrho^T_{g,t,s} = \varrho^{SE}_{t,s} \quad \forall t\in\mathcal{T}, s\in\mathcal{S} \tag{35}$$

$$\sum_{g\in\mathcal{G}_T}\left(\nu^T_{g,t,s}+\varrho^T_{g,t,s}\right) \le \overline{\Gamma^T_t} \quad \forall t\in\mathcal{T}, s\in\mathcal{S} \tag{36}$$

The lower-level optimization problem is formulated to minimize the ISO's costs. The first term of (24) represents the generation costs of transmission-connected assets. The second term refers to the market revenue due to power exchanges with the DSO. Finally, the third term describes the carbon market returns of each transmission-connected generation due to carbon allowance transactions with the DSO. It is important to highlight that the second and third terms present opposite signs compared to (44), which means when one agent profits, the other loses. The transmission system's power balance for nodes without and with an interface with the DS are given in (25) and (26), respectively. The DC power flow is employed to calculate each transmission line's loading (27), as commonly considered in the literature [22, 25]. The power limits of each transmission-connected generator, line, and substation are regarded in (28)–(33). The carbon emission due to transmission-connected conventional generators producing active power is calculated in (34). The transmission system's carbon balance is regarded in (35). Finally, the transmission system's carbon allowance per time period is addressed in (36) [15]. Moreover, variables $\lambda_{i,t,s}$ and $\psi_{t,s}$ (employed in the upper-level objective function formulation) are the dual variables of (26) and (35), respectively. It should be mentioned that variables $\pi^E_{i,t,s}$ and $\pi^C_{t,s}$ are DSO's bids on the electricity and carbon markets. Given that the DSO is the upper-level agent it is able to infer the shadow prices. In this context, submitting a bid that is higher than the shadow price will lead to the offer not being entirely accepted, which limits the agent's profit. On the other hand, submitting a bid cheaper than the nodal price would guarantee its acceptance, but also restrain the revenue. Thus, to attain the optimal solution, the upper-level agent must ensure that their bids are equal to the shadow prices [22].

The emission limits are calculated based on the average of the available generators' carbon intensity and demand, as expressed in (37)–(39). The parameter U is employed to represent different rigidity levels for the carbon emission regulation.

$$\Lambda = \frac{\sum_{g\in\mathcal{G}_T}\overline{P}^T_g\gamma^T_g + \sum_{g\in\mathcal{G}_D}\overline{S}^D_g\gamma^D_g}{\sum_{g\in\mathcal{G}_T}\overline{P}^T_g + \sum_{g\in\mathcal{G}_D}\overline{S}^D_g} \tag{37}$$

$$\overline{\Gamma}^T_t = U\Lambda\sum_{i\in\mathcal{N}_T} L^T_{i,t,s} \quad \forall t\in\mathcal{T}, s\in\mathcal{S} \tag{38}$$

$$\overline{\Gamma}^D_t = U\Lambda\sum_{i\in\mathcal{N}_D} L^D_{i,t,s} \quad \forall t\in\mathcal{T}, s\in\mathcal{S} \tag{39}$$

For the sake of completeness, the BLP-based optimization problem can be expressed as follows:

$$\min \sum_{s\in\mathcal{S}}\sum_{t\in T} p_{s,t}\left[\sum_{g\in\mathcal{G}_D}\sum_{b\in\mathcal{B}_g}\left(C^D_{g,b}\rho^D_{g,b,t,s}\right) + \psi_{t,s}\varrho^{SE}_{t,s} + \sum_{i\in\mathcal{N}_\infty}\lambda_{i,t,s}P^{SE}_{i,t,s}\right] \tag{40}$$

subject to:

Constraints (2)–(23). (41)

$$\{P^{SE}_{i,t,s}, Q^{SE}_{i,t,s}, \varrho^{SE}_{t,s}\} = \arg\min \sum_{s\in\mathcal{S}}\sum_{t\in T} p_{s,t}\left[\sum_{g\in\mathcal{G}_T}\sum_{b\in\mathcal{B}_g}\left(C^T_{g,b}\rho^T_{g,b,t,s}\right) - \pi^C_{t,s}\varrho^{SE}_{t,s} - \sum_{i\in\mathcal{N}_\infty}\pi^E_{i,t,s}P^{SE}_{i,t,s}\right] \tag{42}$$

subject to: Constraints (25)–(36). (43)

The model described in (40)–(43) can be re-written as a single-level model by replacing the lower-level problem with its Karush–Kuhn–Tucker (KKT) conditions [31, 32]. The resulting MPEC model is a nonconvex NLP problem due to the formulations of the market transactions (bilinear terms in the objective function) and the KKT slackness conditions, which can be found in Appendix A. Nonetheless, well-known techniques based on the strong-duality theorem and complementarity constraints can be employed to linearize such terms [22, 28]. The resulting MIQCP formulation that substitutes the original MPEC can be found in Appendix B. Admitedly, the employment of KKT conditions is possible only if the optimization problem modeled in the lower level is continuous and convex, which prohibits the use of well-detailed power flow formulations for the transmission system. Yet, the use of the DC power flow model to represent the operation of transmission systems is common in the literature [22, 25].

3. Numerical Results

The proposed model was validated for modified versions of IEEE 14 and 34-node systems, employed as the transmission and distribution networks, respectively. The DS is connected to transmission node 5. We modified the DS by inserting 8 generators (5 dispatchable and 3 non-dispatchable), 2 ESSs, and 8 controllable loads. Additionally, 3 non-dispatchable renewable-based generators were included in the transmission system, in addition to the existing 5 dispatchable ones. The networks' illustration, as well as their data, are available in [24]. The data for carbon intensity was generated based on the values found in [15, 17]. Nonetheless, the values used in three of the transmission-connected generators (G1, G2, and G3) were multiplied by a factor of up to 3 to represent old power plants with higher carbon intensity. The results presented in this section were obtained considering a 24-hour planning horizon divided into 1h periods.

3.1. Model Validation

Previous research addressed the advantages of formulating the optimal dispatch in a BLP-based manner instead of a centralized approach, as well as the effects of considering E&C trading environments [23]. Nonetheless, the authors have solved the equivalent MPEC in its nonlinear formulation. In this sense, we validate the proposed MIQCP approach (C1) by comparing the results obtained with it and those found by the NLP model proposed in [23] (C2). Additionally, the results obtained by a centralized dispatch formulation (C3) are provided as a benchmark for the two MPEC-based models. The MIQCP and NLP problems were solved, respectively, by Gurobi 11.0.0 [33] and CONOPT [34] both under the mathematical programming language AMPL [35] in an Intel i7-10700 computer at 2.9 GHz with 32 GB of RAM.

It should be mentioned that the model presented in [23] has a deterministic formulation. In this sense, the results shown in this subsection were obtained considering a single scenario. The total operational costs of each agent (DSO and ISO) obtained by each model for the deterministic example and considering $U = 1.00$ are presented in Table 2. It should be pointed out that the market environments do not exist in the centralized formulation. Therefore, the DSO's operational costs are higher as the DSO-ISO transactions are not priced, but the DSO's production costs are. Nonetheless, the centralized formulation provides the minimum production costs, which can be used to highlight how close the MPEC-based dispatches are to the most economical one. It can be observed in Table 2 that, although the NLP-based formulation provides a more economical power dispatch, the MIQCP-based model yields a better market strategy for the DSO. In this sense, since the DSO cost minimization is formulated as the upper-level problem, the solution found by C1 is considerably better than that obtained by C2.

Table 2
Operative Costs Obtained by Each Formulation ($)

	DSO Costs	ISO Costs	Total Production Costs
C3	1,374.18	6,079.28	7,453.46
C2	121.91	7,335.50	7,457.41
C1	-3.61	7,498.46	7,494.85

Note: C1 - Proposed MIQCP model; C2 - NLP model; C3 - Centralized model.

3.2. Sensitivity Analysis of the DSO's Profit

The results featured in this subsection were obtained considering the stochastic formulation described in section 2. The wind- and solar-based generation scenarios were obtained by applying a normal deviation to historical data available in [36]. Uncertainty regarding the demands was represented by applying a normal deviation to the expected demand. 100 scenarios for each hour were randomly generated for each uncertain parameter. Next, the scenario tree was reduced to 5 independent scenarios using the method proposed in [37]. Data regarding the scenarios is available in [24]. It is important to highlight that all of the results presented from this point forward were obtained considering a stochastic formulation, rather than the deterministic one presented in subsection A.

In this subsection, we investigate the DSO's and ISO's profits under different carbon emission regulations. Only the proposed MIQCP-based formulation is regarded in this study. The carbon emission regulation's rigidity is represented by the parameter U (as per (38)–(39)). A lower value indicates a more rigorous scenario and $U = \infty$ is equivalent to removing the carbon emission limits. An illustration of the agents' total operative costs under different carbon emission regulations is presented in Fig. 2.

The results illustrated in Fig. 2 show that the DSO's profit increases as the carbon emission regulation becomes more strict. This happens because the transmission-connected generators with the lowest production costs are

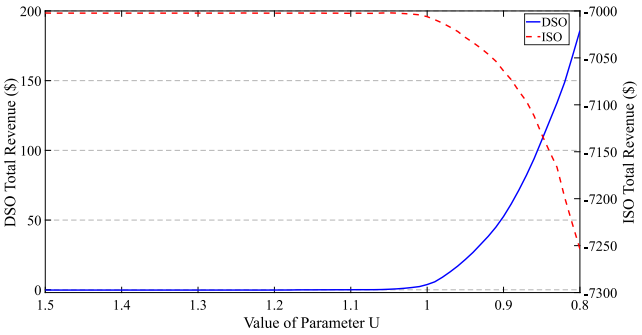

Figure 2: DSO and ISO operative costs under different carbon emission regulations

also amongst the most pollutant units. In this sense, dispatching such power plants becomes challenging as the carbon emission limits decrease. The distributed generators (DGs), on the other hand, are not as cheap to dispatch as the cheapest generator in the transmission system, but are much less pollutant; therefore, being able to dispatch even under the most strict regulation scenario.

The sources of income that contribute to the DSO's profit (i.e., E&C transactions) in different carbon regulation scenarios are shown in Fig. 3. Notably, changes in electricity and carbon market-related revenues are mostly observed for $U \leq 1.05$. It is important to mention that the DSO's profit solely comes from the electricity market, while the carbon market consistently leads to losses. Since the DSO controls the least pollutant energy sources and is formulated as the upper-level problem in the BLP formulation, such behavior, although seemingly counter-intuitive, is a strategic decision. In this sense, this subject is explored in more depth in the next subsection.

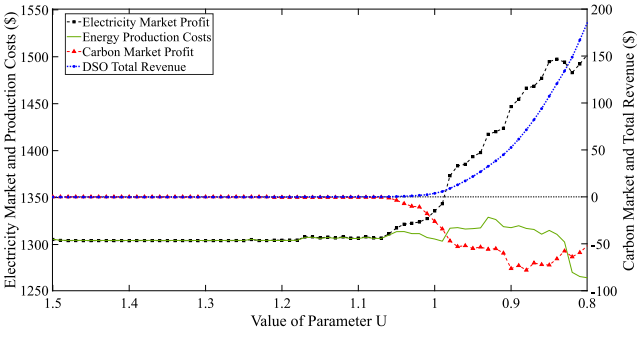

Figure 3: DSO's sources of income under different carbon emission regulations

3.3. Analysis of the DSO's Strategic Behavior

In this subsection, we investigate the DSO's business model, i.e., why the decisions made by this agent lead to its profit maximization. The most straightforward approach is to observe the averages of the markets' hourly clearing prices and power/carbon allowance exchanges between the DSO and the ISO illustrated in Figs. 4 and 5. It can be noticed in Figs. 4(a) and 5(a) that the electricity and carbon allowance prices increase as the carbon emission regulation becomes more strict. It should be mentioned that both power systems are able to supply their demands without trading power with each other, even if $U < 1.00$. However, it would imply the dispatch of more expensive generators. Therefore, it is preferable for both agents to produce electricity with their less expensive generators and trade electricity and carbon allowances in the market environments. Nonetheless, when trading carbon allowances is necessary, the operational cost of a generator is not simply given by its generation cost parameters but also by how much credit must be traded to allow the dispatch of this unit. These new costs are ultimately transferred to the LMPs. That is why the lower the carbon emission limits, the higher the electricity prices. The increase in LMPs justifies the behavior observed in Fig. 3, wherein electricity market profit and production costs tend to increase and decrease, respectively, for $U \to 0.8$. Note in Fig. 4(b), for example, that the DSO trades less electricity when $U = 0.80$ than in any other case; nonetheless, Fig. 3 shows that the DSO presents the highest electricity market profit for this case.

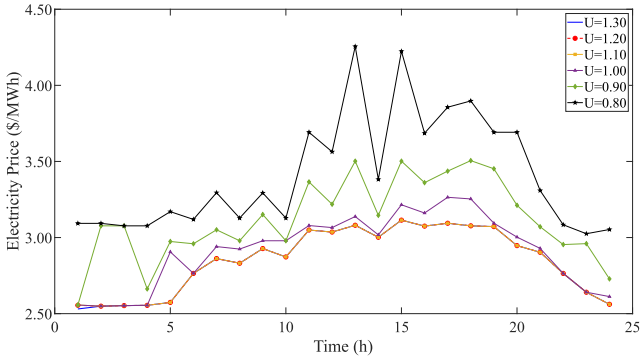

(a) Expected electricity prices

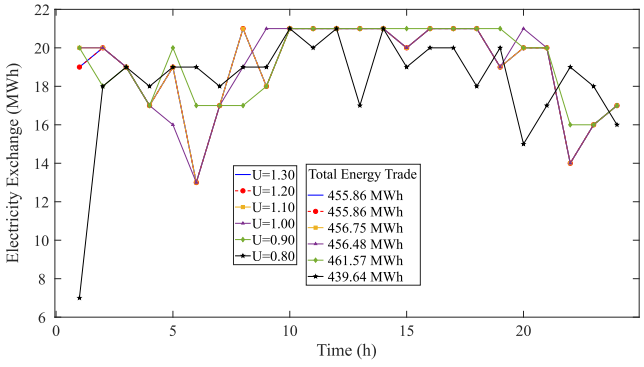

(b) Expected electricity exchanges

Figure 4: DSO's expected operation in the electricity market

Also noteworthy, the electricity prices shown in Fig. 4(a) differ from the baseline value (result for $U = 1.30$) only when the carbon allowance price is greater than zero (check Fig. 5(a)). In this sense, even though Fig. 5(b) shows carbon trades for $U > 1.00$, such transactions are not priced, as can be observed in Fig. 5(a) and, therefore, do not affect the objective function of either agent.

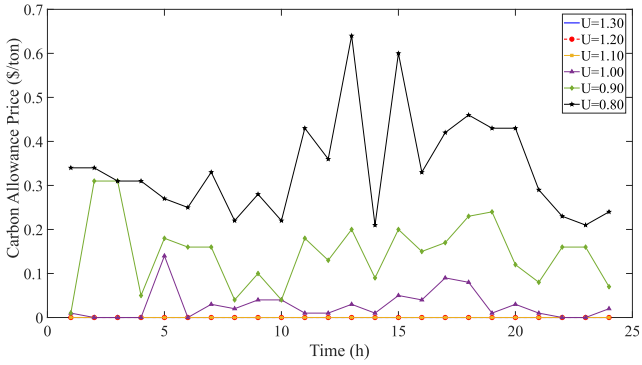

(a) Expected carbon prices

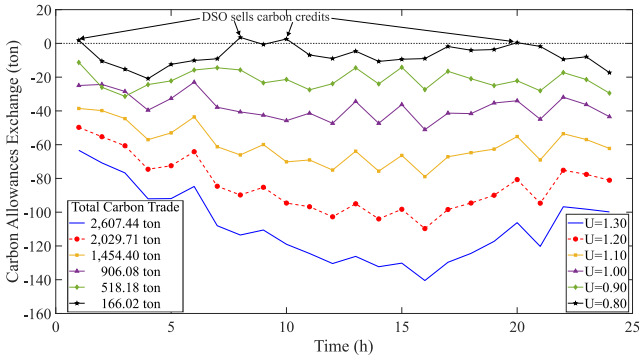

(b) Expected carbon allowance exchanges

Figure 5: DSO's expected operation in the carbon market

Regarding the DSO's transactions on the carbon market environment illustrated in Fig. 5(b), it should be stressed that even though the DSO controls the less pollutant conventional generators, the agent rarely sells carbon allowances in the market. Besides taking losses in the carbon market environment, as shown in Fig. 3, the DSO purchases more carbon allowances than what is produced hourly by its generators. The examination of such a decision was carried out by comparing it with the solutions found in two additional case studies. Case study C4 disregards the possibility of trading carbon allowances, i.e., the agents are only able to trade electricity. Case study C5 allows the agents to trade both electricity and carbon allowances; however, neither agent can purchase more carbon allowances than the amount of greenhouse gasses produced by their generators. The operative costs obtained for each case study, considering $U = 1.00$ and a deterministic formulation that allows a better understanding of each power source's behavior, are presented in Table 3 wherein it is possible to verify that indeed purchasing more carbon allowances than needed enhances the DSO's profit.

Next, we investigate why purchasing additional carbon allowances benefits the DSO. In this sense, Fig. 6(a) shows the contribution of each power source to the energy matrix for every case study, while Fig. 6(b) illustrates the agents' daily carbon emissions. Observe that as the carbon market environment becomes more deregulated, the ISO carbon emissions tend to reduce, and the opposite happens to the DSO. Simultaneously, the contributions of generators 1, 2, 3, and 4 to the energy matrix decrease as the DSO's participation increase. It is important to highlight that generators G1 and G2 are the cheapest and most pollutant transmission-connected sources. Thus, such power plants tend to inject less power when the ISO sells carbon allowances to the DSO since selling carbon allowances and dispatching these units would quickly deplete the ISO carbon emission quota forcing the agent to buy more electricity in the wholesale market.

Table 3
Overall Costs of Each Case Study ($)

	DSO Costs	ISO Costs	Total Generation Costs
C4	157.53	6,960.61	7,118.14
C5	84.71	6,979.46	7,064.17
C1	3.17	7,022.81	7,025.98

Note: C1 - Proposed model with an unconstrained carbon market environment; C4 - Case study without the carbon market environment; C5 - Case study with carbon market environment and additional purchase constraint.

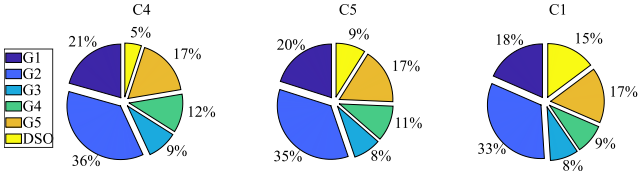

(a) Energy matrix for each case study

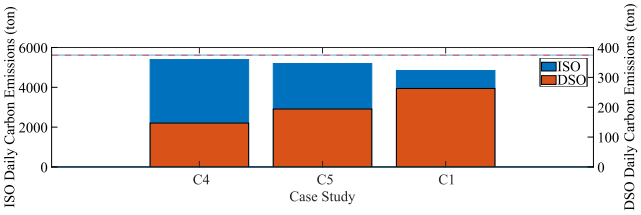

(b) DSO and ISO daily carbon emissions for each case study

Figure 6: Wholesale energy and carbon matrices

On the other hand, if the cheapest power sources produce less electricity, more onerous units must be dispatched, which leads to increasing the wholesale market's clearing price, as can be observed in Fig. 7. Observe that the clearing prices are lower when carbon trades, even if regulated, are permitted (i.e., case C5) compared to the prices without carbon trades. This happens because when carbon trades are prohibited, the most expensive transmission-connected generators are dispatched, which increases the market clearing price. Additionally, notice for C1 that whenever the DSO purchases more carbon allowances than needed[1] there is an electricity price spike in comparison to those of C4 and C5 (except for the hours highlighted in purple, namely hours 9, 13 and 21). The electricity price spikes are the result

[1] Represented by $\Delta\text{Expense}_{\text{carbon market}}$, which is defined as the difference between the carbon market hourly costs of C5 and C1. Since C5 has a regulated carbon trade environment in which the DSO cannot purchase more carbon allowances than it is capable of using, the unused carbon allowances can be calculated by subtracting the hourly C5 purchases from C1's.

of the DSO's strategic behavior of purchasing carbon allowances that lead to the reduction of the power dispatch of cheap and pollutant transmission generators. Ultimately, this causes less pollutant and more expensive transmission-connected units to dispatch, which increases the market clearing price. The electricity price spikes cause the DSO to profit more from the electricity market, which is represented by $\Delta\text{Expense}_{\text{electricity market}}$. It is worth mentioning that the additional gains from the electricity market surpass the additional expenses in the carbon market, which yields a substantial benefit to the DSO's objective function (97.99% reduction in comparison with C4 and 96.26% reduction in comparison with C5) at the expense of slightly worsening the ISO's (0.89% increase in comparison with C4 and 0.62% increase in comparison with C5), as shown in Table 3.

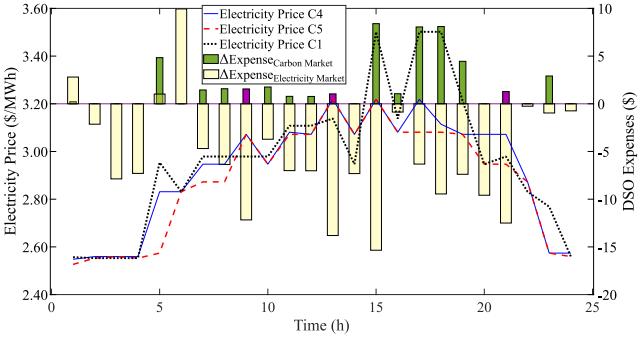

Figure 7: Impact of strategic bidding on the DSO's hourly revenues

3.4. Optimal Asset Management

In this subsection, we investigate the correlation between the hourly wholesale electricity price and the management of DS-connected assets for case study C1. An illustration of the hourly dispatch of each type of DER, as well as the total power exported by the DS, is provided in Fig. 8. Observe in Fig. 8(a) that the DSO uses the DR to shift load away from the period comprised between hours 16 and 21 since the expected electricity price is high during these hours. The demand is shifted mainly to the period comprising hours 4 to 15. Additionally, it is possible to observe that the correlation between the expected clearing price and the power exchange ($\boldsymbol{P}^{SE}$) is not strong.

The reason why the DSO's power injection into the transmission system is somewhat constant between 9h and 18h regardless of the price variations also justifies the seeming lack of correlation between the expected power exchange and electricity price. The DS-connected conventional generators have such production costs that for a \$2.55/MWh clearing price, generating a total 31.7MW divided among the units is profitable[2]. Nonetheless, the total conventional-based electricity production, which accounts for most of the DS generation capacity[3], does not surpass 30.1MW (see Fig. 8(b)) during the entire planning horizon even though the prices are greater than \$2.55/MWh. In this sense, it is possible to conclude that the power exchange is limited not by the clearing price but due to the DS's operative limits. Further study shows that the voltage magnitude at node 34 (where DG5 is located) is 1.05 p.u. during the entire planning horizon for every scenario.

Since electricity price is not what limits the power exchange, the conventional units' hourly dispatch does not vary much, as can be observed in Fig. 8(b). Nonetheless, slight changes must be made to accommodate load and renewable power variations. The hourly dispatch changes for every conventional DG are presented in Fig. 8(c), wherein it is possible to observe that DG4 injects the same amount of power throughout the planning horizon as this is the cheapest conventional power plant in the DS. DGs 1 and 2 are the next least expensive sources and, as such, experience less significant changes in power dispatch than DG 3 and 5.

Fig. 8(d) shows the contributions of DR[4], ESSs, and renewable-based generation to the power exchange. It should be mentioned that given that the electricity price is not limiting the power exchange between DSO and ISO, the wholesale electricity market's clearing price is determined by transmission-connected generators. Thus, the price oscillation behavior observed in Fig. 8 is not caused by the DS (although the magnitude is potentiated by the DSO's strategic bids as discussed in the previous subsection). In this sense, the DR, ESSs behavior represents the DSO's reaction to the clearing price. It is possible to observe that the ESSs tend to charge before 10h and after 21h, i.e., charge during off-peak prices and discharge during peak prices. The load-shifting behavior is similar, but since the hourly demand limits the load-shift magnitude, additional hours of negative contribution are needed to allow a more significant contribution during the period comprised between hours 16 and 21.

Finally, it is important to address the DR and ESSs behavior during hours 1, 2, 3, 22, 23, and 24. Even though electricity prices are higher during the three final hours of the planning horizon than in the first three ones (highlighted in Fig. 8(d)), DR and ESSs provide a negative contribution to the power exchange when the prices are higher. We highlight two causes for this behavior. Firstly, it should be stressed that the DSO must control its assets not only to attain profit, given that its most fundamental role is to ensure the DS's safe operation, which may be attained by changing the hourly demand. Furthermore, the ESSs must ensure that the initial and final SOC for the planning horizon are equal. Thus, since the ESSs depleted almost completely their SOC, charging in the last three hours is mandatory.

3.5. Scalability Analysis

The problem was also solved considering a DS composed of 123 nodes instead of the 34-node test system adopted in the previous subsections to assess the scalability of

[2]Data and figures that support this claim are provided in [24].

[3]Compare the right-hand side magnitudes of Figs. 8(a), 8(b), and 8(d) and observe that the order of magnitude in the last one is much smaller, which means renewable, storage systems and load-shift represent a smaller portion of $\boldsymbol{P}^{SE}$ than the conventional generators.

[4]The DR impact on the P^{SE} is opposite in sign to the actual controllable loads' behavior, i.e., a positive DR impact on the P^{SE} means load reduction (negative variation of the original load).

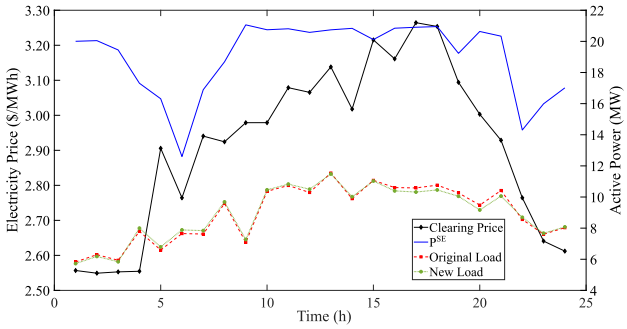

(a) Correlation between expected power exchange and electricity price

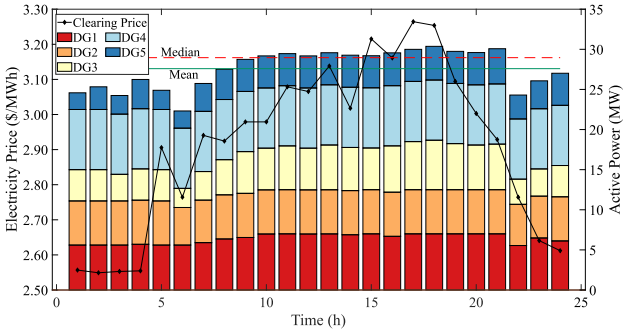

(b) Correlation between expected conventional-based power injection and electricity price

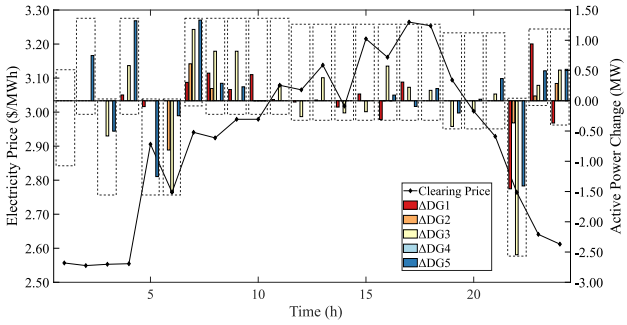

(c) Expected hourly changes in conventional-based power injection

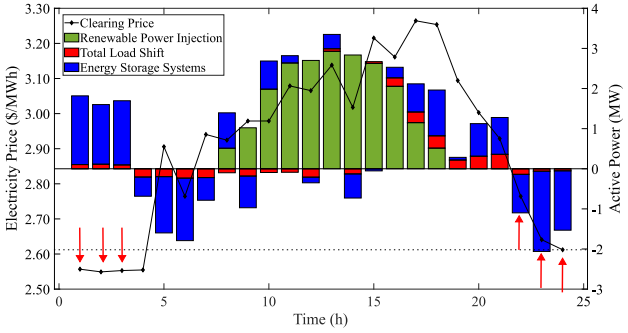

(d) Correlation between expected renewable-based power injection, demand response and electricity price

Figure 8: Optimal management of distribution-connected resources

the proposed model. Besides the greater number of nodes (more than three times as many), the larger DS has 10 DGs (twice as many as the 34-node system), 16 PVs (three times as many as the 34-node system), 25 controllable loads (three times as many as the 34-node system), and 6 ESSs (three times as many as the 34-node system). Data regarding the characteristics of each of these elements, as well as the DS's physical parameters, can be found in [24]. The problem was solved to optimality, and a comparison between the two test systems from a computational burden perspective is shown in Table 4.

Table 4
Computational Effort Analysis

DS Size	CPU Time (s)	# Variables	# Constraints
34 Nodes	1,209.53	12,888	22,378
123 Nodes	5,562.34*	23,856	44,071

* A solution within a 1% gap to optimality can be found in 4,197 s.

A breakdown of the DSO's sources of income and overall operational costs is presented in Table 5. Observe that the DSO has a negative revenue trading carbon allowances even though the less carbon-intense generators are connected to the DS, which is consistent with the results obtained for the smaller distribution network. Thus, adopting the strategy of manipulating the electricity market clearing price by buying unneeded carbon allowances is the optimal course of action for the strategic price-maker (i.e., DSO) in this case study.

Table 5
Overall Costs for the 123-Node DS

Aspect	Value ($)
DSO electricity market Revenue	155.01
DSO Carbon Market Revenue	-0.52
DSO Generation Costs	192.17
DSO Total Operational Costs	37.68
ISO Total Operational Costs	6,931.79
Total Generation Costs	6,969.48

Finally, the electricity market clearing price, as well as the power exchange between the DSO and the ISO, is shown in Fig. 9. It can be extracted from the chart that the electricity clearing price has a similar pattern to that observed for the case study with the 34-node DS, although the values are not the same, and the price behavior sometimes does not match due to the different characteristics (i.e., demand and load profile) of the DSs. Furthermore, the power exchange tends to follow the clearing price. However, after hour 16, the power exchange is substantially reduced even though the clearing price decreases at a lower rate. Such behavior is due to physical limits of the DS, which was also observed for the 34-node DS and discussed in more details in section 3.4.

4. Conclusion

In this paper, we address the strategic bidding of a DSO participating in the E&C wholesale day-ahead market environment. The DSO must optimally manage controllable

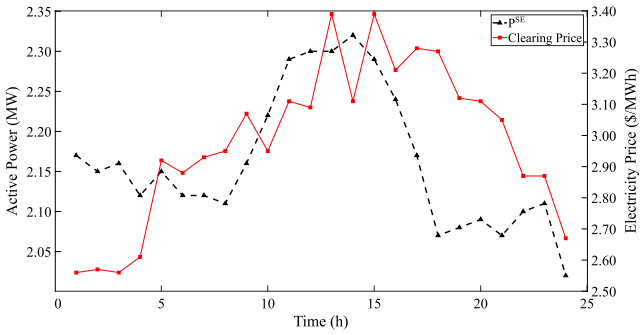

Figure 9: DSO's expected operation in the electricity market for the 123-node DS

assets connected to the DS to ensure maximum profit from the market environment. A stochastic formulation is employed to address the uncertainties related to demand and renewable power availability. The problem is formulated as a BLP in which maximizing the DSO's profit is the upper-level problem while clearing the markets and operating the transmission system is the lower-level problem. Power flow constraints to ensure the safe operation of both transmission and distribution systems are considered in the upper- and lower-level problems. The BLP is rewritten as a MPEC and then transformed into a MIQCP for which finite convergence to the optimal solution is guaranteed.

Numerical results reveal the superiority of the proposed approach over an existing nonlinear formulation. Additionally, a sensitivity analysis of the DSO's profit sources shows that a more strict carbon emission regulation implies a higher payoff, which is caused only by the carbon trades. This result is supported by the fact that a more strict carbon emission hinders the dispatch of less expensive (but highly pollutant) generators, thus, affecting electricity prices. As a result, the DSO has higher profitability in the electricity market.

Another core finding is the nuances of the DSO's strategic behavior in the E&C environments that include bidding in the carbon market, even though the DS-connected generators are less pollutant, thus rendering the DSO able to offer carbon allowances instead of buying them. The investigation conducted on this subject shows that it is beneficial to the DSO to bid in carbon allowances since, due to this action, the ISO dispatches more expensive power sources to simultaneously sell carbon allowances to the DSO and guarantee power balance in the transmission system. In this context, the DSO increases its profits from the electricity market due to the higher LMPs enough to compensate for the loss in the carbon market environment. Finally, the hourly dispatch of each DS-connected DER is presented to attest to the DSO's optimal management of its assets. Although the DS is congested throughout the planning horizon, the DERs respond to the price signal accordingly.

Future work may focus on modeling a more complex market framework wherein more agents are considered. Including this feature could lead to a multi-leader bilevel formulation for which General Nash Equilibrium should be proved if a centralized solving technique is employed. Alternatively, decentralized approaches could be used to avoid the Nash Equilibrium verification at the expense of not guaranteeing the solution's optimality. Another possibility to improve the proposed model is to enhance the transmission system power flow model to account for the reactive power flow and nodal voltages. Finally, an additional optimization layer could be included to properly represent the distribution-level E&C market environments.

Acknowledgments

The work of W. R. Faria and B. R. Pereira Jr. was supported in part by CAPES – Finance Code 001, and in part by FAPESP under Grant 2021/04628-0. The work of G. Muñoz-Delgado and J. Contreras was supported in part by Grant PID2021-122579OB-I00 funded by the Junta de Comunidades de Castilla-La Mancha, by the Spanish Ministry of Finance and Civil Service, by European Union Funds, and by the ERDF, and in part by grant 2023-GRIN-34074, funded by the Universidad de Castilla-La Mancha, under the UCLM Research Group Program, and by the European Commission, under the ERDF.

Appendix

In this section, we present the MPEC reformulation of the bilevel optimization problem presented in (40)–(43). Additionally, the linearization methods employed to transform the nonlinear MPEC formulation into a MIQCP model are also explained in this section.

Nomenclature

In this subsection, additional variables related to the lower-level dual problem are defined.

$\overline{\alpha}_{g,t,s}$	Dual variable associated with the upper bound for the power injection of transmission-connected generators (eq. 28/29).
$\underline{\alpha}_{g,t,s}$	Dual variable associated with the lower bound for the power injection of transmission-connected generators (eq. 28/29).
$\overline{\rho}_{g,b,t,s}$	Dual variable associated with the upper bound for the accepted bids of transmission-connected generators (eq. 31).
$\underline{\rho}_{g,b,t,s}$	Dual variable associated with the lower bound for the accepted bids of transmission-connected generators (eq. 31).
$\overline{\omega}_{l,t,s}$	Dual variable associated with the upper bound for the power flow across transmission lines (eq. 32).
$\underline{\omega}_{l,t,s}$	Dual variable associated with the lower bound for the power flow across transmission lines (eq. 32).
$\overline{\kappa}_{i,t,s}$	Dual variable associated with the upper bound for the substations' capacities (eq. 33).
$\underline{\kappa}_{i,t,s}$	Dual variable associated with the lower bound for the substations' capacities (eq. 33).
$\lambda_{i,t,s}$	Dual variable associated with the power balance at transmission nodes (eq. 25/26).
$\mu_{l,t,s}$	Dual variable associated with the transmission system power flow calculation (eq. 27).
$\psi_{t,s}$	Dual variable associated with the transmission system's carbon balance (eq. 35).

$\phi_{g,t,s}$ Dual variable associated with the transmission-connected generators' carbon emissions (eq. 34).

$\varphi_{g,t,s}$ Dual variable associated with the sum of the transmission-connected generators' accepted bids (eq. 30).

$\xi_{t,s}$ Dual variable associated with the transmission system's carbon allowance limit (eq. 36).

A. Reformulation as a MPEC

As a general rule, adopting the strong duality theorem to formulate the MPEC model leads to lower computational burden than using KKT conditions, as shown in [32]. However, for this specific problem, the linearization of the bilinear terms in the leader's objective function has an even heavier computational effort than the KKT conditions if the primal-dual model is employed to describe the MPEC model, as observed in [22, 28]. Thus, the MPEC model is formulated using KKT conditions as follows.

$$\min \sum_{s\in\mathcal{S}}\sum_{t\in\mathcal{T}} p_{s,t}\left[\sum_{g\in\mathcal{G}_D}\sum_{b\in\mathcal{B}_g}\left(C^D_{g,b}\rho^D_{g,b,t,s}\right) + \psi_{t,s}\varrho^{SE}_{t,s} + \sum_{i\in\mathcal{N}_\infty}\lambda_{i,t,s}P^{SE}_{i,t,s}\right] \tag{44}$$

subject to:

Constraints (2)–(23): Upper-level constraints (45)

Constraints (25)–(36): ISO's primal constraints (46)

$$-\sum_{i\in\mathcal{N}_T\cap\mathcal{G}_T}\left(\lambda_{i,t,s}\right) - \phi_{g,t,s}\gamma^T_g + \overline{\alpha}_{g,t,s} - \underline{\alpha}_{g,t,s} + \varphi_{g,t,s} = 0 \quad \forall g\in\mathcal{G}_T, t\in\mathcal{T}, s\in\mathcal{S} \tag{47}$$

$$C^T_{g,b} - \varphi_{g,t,s} + \overline{\rho}_{g,b,t,s} - \underline{\rho}_{g,b,t,s} = 0 \quad \forall g\in\mathcal{G}_T, b\in\mathcal{B}_g, t\in\mathcal{T}, s\in\mathcal{S} \tag{48}$$

$$-\sum_{l\in\mathcal{L}_T}\left(\frac{A_{i,l}\mu_{l,t,s}}{X_l}\right) = 0 \quad \forall i\in\mathcal{N}_T\cup\mathcal{N}_\infty, t\in\mathcal{T}, s\in\mathcal{S} \tag{49}$$

$$\mu_{l,t,s} + \overline{\omega}_{l,t,s} - \underline{\omega}_{l,t,s} - \sum_{i\in\mathcal{N}_T\cup\mathcal{N}_\infty} A_{i,l}\lambda_{i,t,s} = 0 \quad \forall l\in\mathcal{L}_T, t\in\mathcal{T}, s\in\mathcal{S} \tag{50}$$

$$-\pi^E_{i,t,s} + \lambda_{i,t,s} + \overline{\kappa}_{i,t,s} - \underline{\kappa}_{i,t,s} = 0 \quad \forall i\in\mathcal{N}_\infty, t\in\mathcal{T}, s\in\mathcal{S} \tag{51}$$

$$\phi_{g,t,s} + \overline{\xi}_{t,s} = 0 \quad \forall g\in\mathcal{G}_T, t\in\mathcal{T}, s\in\mathcal{S} \tag{52}$$

$$\psi_{t,s} + \overline{\xi}_{t,s} = 0 \quad \forall g\in\mathcal{G}_T, t\in\mathcal{T}, s\in\mathcal{S} \tag{53}$$

$$\pi^C_{t,s} - \psi_{t,s} = 0 \quad \forall t\in\mathcal{T}, s\in\mathcal{S} \tag{54}$$

$$\overline{\alpha}_{g,t,s}(-P^T_{g,t,s} + \overline{P}^T_g) = 0 \quad \forall g\in\mathcal{G}_T, t\in\mathcal{T}, s\in\mathcal{S} \tag{55}$$

$$\underline{\alpha}_{g,t,s}(P^T_{g,t,s}) = 0 \quad \forall g\in\mathcal{G}_T, t\in\mathcal{T}, s\in\mathcal{S} \tag{56}$$

$$\overline{\omega}_{l,t,s}(-PF_{l,t,s} + \overline{PF}_l) = 0 \quad \forall l\in\mathcal{L}_T, t\in\mathcal{T}, s\in\mathcal{S} \tag{57}$$

$$\underline{\omega}_{l,t,s}(PF_{l,t,s} + \overline{PF}_l) = 0 \quad \forall l\in\mathcal{L}_T, t\in\mathcal{T}, s\in\mathcal{S} \tag{58}$$

$$\overline{\rho}_{g,b,t,s}(-\rho^T_{g,b,t,s} + \overline{P}^T_{g,b}) = 0 \; \forall g\in\mathcal{G}_T, b\in\mathcal{B}_g, t\in\mathcal{T}, s\in\mathcal{S} \tag{59}$$

$$\underline{\rho}_{g,b,t,s}(\rho^T_{g,b,t,s}) = 0 \quad \forall g\in\mathcal{G}_T, b\in\mathcal{B}_g, t\in\mathcal{T}, s\in\mathcal{S} \tag{60}$$

$$\overline{\kappa}_{i,t,s}(-P^{SE}_{i,t,s} + \overline{P}^{SE}_i) = 0 \quad \forall i\in\mathcal{N}_\infty, t\in\mathcal{T}, s\in\mathcal{S} \tag{61}$$

$$\underline{\kappa}_{i,t,s}(P^{SE}_{i,t,s} + \overline{P}^{SE}_i) = 0 \quad \forall i\in\mathcal{N}_\infty, t\in\mathcal{T}, s\in\mathcal{S} \tag{62}$$

$$\xi_{t,s}\left(\overline{\Gamma}^T_t - \sum_{g\in\mathcal{G}_T}\left(\nu^T_{g,t,s} + \varrho^T_{g,t,s}\right)\right) = 0 \quad \forall t\in\mathcal{T}, s\in\mathcal{S} \tag{63}$$

$$\overline{\alpha}_{g,t,s} \geq 0 \qquad \underline{\alpha}_{g,t,s} \geq 0 \quad \forall g\in\mathcal{G}_T, t\in\mathcal{T}, s\in\mathcal{S} \tag{64}$$

$$\overline{\rho}_{g,b,t,s} \geq 0 \qquad \underline{\rho}_{g,b,t,s} \geq 0 \quad \forall g\in\mathcal{G}_T, b\in\mathcal{B}_g, t\in\mathcal{T}, s\in\mathcal{S} \tag{65}$$

$$\overline{\kappa}_{i,t,s} \geq 0 \qquad \underline{\kappa}_{i,t,s} \geq 0 \quad \forall i\in\mathcal{N}_\infty, t\in\mathcal{T}, s\in\mathcal{S} \tag{66}$$

$$\overline{\omega}_{l,t,s} \geq 0 \qquad \underline{\omega}_{l,t,s} \geq 0 \quad \forall l\in\mathcal{L}_T, t\in\mathcal{T}, s\in\mathcal{S} \tag{67}$$

$$\xi_{t,s} \geq 0 \qquad \forall t\in\mathcal{T}, s\in\mathcal{S} \tag{68}$$

Equations (47)–(54) are the KKT stationary conditions, while equations (55)–(63) represents the complementary slackness conditions. Finally (64)–(68) are the dual feasibility constraints.

B. Mixed-Integer Quadratically Constrained Formulation

The nonlinear equations described in (55)–(63) can be linearized using the Big-M method. An example is presented for (55), which is rewritten as (69)–(70). The same procedure is applied to the other complementary slackness equations.

$$\overline{\alpha}_{g,t,s} \leq M z^{\overline{\alpha}}_{g,t,s} \quad \forall g\in\mathcal{G}_T, t\in\mathcal{T}, s\in\mathcal{S} \tag{69}$$

$$(-P^T_{g,t,s} + \overline{P}^T_g) \leq M(1 - z^{\overline{\alpha}}_{g,t,s}) \quad \forall g\in\mathcal{G}_T, t\in\mathcal{T}, s\in\mathcal{S} \tag{70}$$

being $z^{\overline{\theta}}$ a binary variable that indicates that the constraint $P^T_{g,t,s} \leq \overline{P}^T_g$ is active, i.e., $P^T_{g,t,s} = \overline{P}^T_g$. M is a sufficiently large constant.

As for the linearization of the bilinear terms in (44), namely $(\psi_{t,s}\varrho^{SE}_{t,s})$ and $(\lambda_{i,t,s}P^{SE}_{i,t,s})$, the following steps were taken.

From the strong duality theorem, we know that the primal and dual objective functions of an optimization problem assume the same value at the optimal solution. Thus, applying the strong duality theorem for the ISO model, one can write the following equation.

$$\sum_{s\in S}\sum_{t\in\mathcal{T}} p_{s,t}\left[\sum_{g\in\mathcal{G}_T}\sum_{b\in\mathcal{B}_g}\left(C^T_{g,b}\rho^T_{g,b,t,s}\right) - \pi^C_{t,s}\varrho^{SE}_{t,s} - \sum_{i\in\mathcal{N}_\infty}\pi^E_{i,t,s}P^{SE}_{i,t,s}\right] = \sum_{i\in\mathcal{N}_T}\lambda_{i,t,s}L^T_{i,t,s} - \sum_{l\in\mathcal{L}_T}PF_l\left(\overline{\omega}_{l,t,s}+\underline{\omega}_{l,t,s}\right) - \sum_{g\in\mathcal{G}_T,b\in\mathcal{B}_g}\overline{\rho}_{g,b,t,s}\overline{P}^T_{g,b} - \xi_{t,s}\Gamma^T_t - \sum_{i\in\mathcal{N}_\infty}\overline{P}^{SE}_i\left(\overline{\kappa}_{i,t,s}+\underline{\kappa}_{i,t,s}\right) \tag{71}$$

Henceforth, the right-hand side of (71) will be referred to as **B**. Observe that **B** is a linear function. Thus, $\pi^E_{t,s}P^{SE}_{i,t,s} + \pi^C_{t,s}\varrho^{SE}_{t,s}$ can be written as:

$$\sum_{s\in S}\sum_{t\in\mathcal{T}} p_{s,t}\left(\pi^C_{t,s}\varrho^{SE}_{t,s} + \sum_{i\in\mathcal{N}_\infty}\pi^E_{i,t,s}P^{SE}_{i,t,s}\right) = -\mathbf{B} + \sum_{s\in S}\sum_{t\in\mathcal{T}} p_{s,t}\sum_{g\in\mathcal{G}_T}\sum_{b\in\mathcal{B}_g}\left(C^T_{g,b}\rho^T_{g,b,t,s}\right) \tag{72}$$

Thus, the problem can be written in its MIQCP formulation as:

$$\min \sum_{s\in S}\sum_{t\in T} p_{s,t}\left[\sum_{g\in\mathcal{G}_D}\sum_{b\in\mathcal{B}_g}\left(C^D_{g,b}\rho^D_{g,b,t,s}\right) + \sum_{g\in\mathcal{G}_T}\sum_{b\in\mathcal{B}_g}\left(C^T_{g,b}\rho^T_{g,b,t,s}\right)\right] - \mathbf{B} \tag{73}$$

subject to:

$$\text{Constraints (45)–(68)(adopting linear formulations shown in (69)–(70) for constraints (55)–(63))} \tag{74}$$

References

[1] United Nations. Stockholm Conference, 1972. URL https://www.un.org/en/conferences/environment/stockholm1972.

[2] United Nations. Paris Agreement, 2015. URL https://unfccc.int/sites/default/files/english_paris_agreement.pdf.

[3] European Environment Agency. The EU Emissions Trading System in 2019: trends and projections, 2019. URL https://www.eea.europa.eu/publications/the-eu-emissions-trading-system.

[4] European Environment Agency. EU Emissions Trading System (ETS) data viewer, 2023. URL https://www.eea.europa.eu/data-and-maps/dashboards/emissions-trading-viewer-1.

[5] Ciniro Aparecido Leite Nametala, Wandry Rodrigues Faria, Guilherme Guimarães Lage, and Benvindo Rodrigues Pereira. Analysis of hourly price granularity implementation in the Brazilian deregulated electricity contracting environment. *Util. Policy*, 81, Apr. 2023. ISSN 0957-1787. doi: https://doi.org/10.1016/j.jup.2023.101513. art. no. 101513.

[6] California Air Resources Board. Cap-and-Trade Program. URL https://ww2.arb.ca.gov/our-work/programs/cap-and-trade-program.

[7] European Union. EU Emissions Trading System. URL https://climate.ec.europa.eu/eu-action/eu-emissions-trading-system-eu-ets_en.

[8] Houyu He, Zhao Luo, Qian Wang, Maoxin Chen, Huaqin He, Lingjun Gao, and Haixiang Zhang. Joint operation mechanism of distributed photovoltaic power generation market and carbon market based on cross-chain trading technology. *IEEE Access*, 8:66116–66130, Apr. 2020. doi: 10.1109/ACCESS.2020.2985577.

[9] Yunqi Wang, Jing Qiu, and Yuechuan Tao. Optimal power scheduling using data-driven carbon emission flow modelling for carbon intensity control. *IEEE Trans. Power Sys.*, 37(4):2894–2905, Jul. 2022. doi: 10.1109/TPWRS.2021.3126701.

[10] Tao Jiang, Hongwei Deng, Linquan Bai, Rufeng Zhang, Xue Li, and Houhe Chen. Optimal energy flow and nodal energy pricing in carbon emission-embedded integrated energy systems. *CSEE J. Power Energy Syst.*, 4(2):179–187, Jun. 2018. doi: 10.17775/CSEEJPES.2018.00030.

[11] Junhong Hao, Qun Chen, Shunjiang Wang, and Kai Gao. Optimal day-ahead scheduling for distributed cleaning heating system with minimal carbon emissions. presented at the IEEE International Electrical and Energy Conference, Nangjing, China, May 2022.

[12] Alireza Akbari-Dibavar, Behnam Mohammadi-Ivatloo, Kazem Zare, Tohid Khalili, and Ali Bidram. Economic-emission dispatch problem in power systems with carbon capture power plants. *IEEE Trans. Ind. Appl.*, 57(4):3341–3351, Jul.-Aug. 2021. doi: 10.1109/TIA.2021.3079329.

[13] Weiqi Hua, Jing Jiang, Hongjian Sun, and Jianzhong Wu. A blockchain based peer-to-peer trading framework integrating energy and carbon markets. *Appl. Energy*, 279, Art. no. 115539, Dec. 2020. ISSN 0306-2619. doi: https://doi.org/10.1016/j.apenergy.2020.115539.

[14] Mingyu Yan, Mohammad Shahidehpour, Ahmed Alabdulwahab, Abdullah Abusorrah, Niroj Gurung, Honghao Zheng, Oladipupo Ogunnubi, Aleksandar Vukojevic, and Esa Aleksi Paaso. Blockchain for transacting energy and carbon allowance in networked microgrids. *IEEE Trans. Smart Grid*, 12(6):4702–4714, Nov. 2021. doi: 10.1109/TSG.2021.3109103.

[15] Zelong Lu, Linquan Bai, Jianxue Wang, Jingdong Wei, Yunpeng Xiao, and Yang Chen. Peer-to-peer joint electricity and carbon trading based on carbon-aware distribution locational marginal pricing. *IEEE Trans. Power Sys.*, 38(1):835–852, Jan. 2023. doi: 10.1109/TPWRS.2022.3167780.

[16] Yunqi Wang, Jing Qiu, Yuechuan Tao, and Junhua Zhao. Carbon-oriented operational planning in coupled electricity and emission trading markets. *IEEE Trans. Power Syst.*, 35(4):3145–3157, Jul. 2020. doi: 10.1109/TPWRS.2020.2966663.

[17] Yunqi Wang, Jing Qiu, Yuechuan Tao, Xian Zhang, and Guibin Wang. Low-carbon oriented optimal energy dispatch in coupled natural gas and electricity systems. *Appl. Energy*, 280, Art. no. 115948:1–20, Dec. 2020. ISSN 0306-2619. doi: https://doi.org/10.1016/j.apenergy.2020.115948.

[18] Xin Cheng, Yun Zheng, Yong Lin, Lei Chen, Yunqi Wang, and Jing Qiu. Hierarchical operation planning based on carbon-constrained locational marginal price for integrated energy system. *Int. J. Electr. Power Energy Syst.*, 128, Art. no. 106714, Jun. 2021. ISSN 0142-0615. doi: https://doi.org/10.1016/j.ijepes.2020.106714.

[19] Yaohua Cheng, Ning Zhang, Baosen Zhang, Chongqing Kang, Weimin Xi, and Mengshuang Feng. Low-carbon operation of multiple energy systems based on energy-carbon integrated prices. *IEEE Trans. Smart Grid*, 11(2):1307–1318, Mar. 2020. doi: 10.1109/TSG.2019.2935736.

[20] Farzad Hassanzadeh Moghimi and Taghi Barforoushi. A short-term decision-making model for a price-maker distribution company in wholesale and retail electricity markets considering demand response and real-time pricing. *Int. J. Electr. Power Energy Syst.*, 117, May 2020. ISSN 0142-0615. doi: https://doi.org/10.1016/j.ijepes.2019.105701. art. no. 105701.

[21] P. Sheikhahmadi, S. Bahramara, J. Moshtagh, and M. Yazdani Damavandi. A risk-based approach for modeling the strategic behavior of a distribution company in wholesale energy market. *Appl. Energy*, 214:24–38, Mar. 2018. ISSN 0306-2619. doi: https://doi.org/10.1016/j.apenergy.2018.01.051.

[22] Salah Bahramara, Pouria Sheikhahmadi, Andrea Mazza, Gianfranco Chicco, Miadreza Shafie-khah, and João P. S. Catalão. A risk-based decision framework for the distribution company in mutual interaction with the wholesale day-ahead market and microgrids. *IEEE Trans. Industr. Inform.*, 16(2):764–778, Feb. 2020. doi: 10.1109/TII.2019.2921790.

[23] Wandry R. Faria, Gregorio Muñoz-Delgado, Javier Contreras, and Benvindo R. Pereira. Optimal management of distribution-connected assets operating under carbon and energy day-ahead markets. In

2023 IEEE Belgrade PowerTech, pages 1–6, 2023. doi: 10.1109/PowerTech55446.2023.10202949.

[24] W. R. Faria, G. Muñoz-Delgado, J. Contreras, and B. R. Pereira Jr. Electronic companion – distribution and transmission coordinated dispatch under joint electricity and carbon day-ahead markets, March 2024. URL https://doi.org/10.5281/zenodo.10845640.

[25] Yahya Kabiri Renani, Mehdi Ehsan, and Mohammad Shahidehpour. Optimal transactive market operations with distribution system operators. *IEEE Trans. Smart Grid*, 9(6):6692–6701, Nov. 2018. doi: 10.1109/TSG.2017.2718546.

[26] Shay Bahramirad, Amin Khodaei, and Ralph Masiello. Distribution markets. *IEEE Power and Energy Magazine*, 14(2):102–106, Apr. 2016. doi: 10.1109/MPE.2016.2543121.

[27] Wandry R. Faria, Gregorio Muñoz-Delgado, Javier Contreras, and Benvindo R. Pereira Junior. A novel framework for the day-ahead market clearing process featuring the participation of distribution system operators and a hybrid pricing mechanism. *Int. J. Electr. Power Energy Syst.*, 155, Art. no. 109664, 2024. ISSN 0142-0615. doi: https://doi.org/10.1016/j.ijepes.2023.109664.

[28] Amir Naebi Toutounchi, Seyedjalal Seyedshenava, Javier Contreras, and Adel Akbarimajd. A stochastic bilevel model to manage active distribution networks with multi-microgrids. *IEEE Syst. J.*, 13(4):4190–4199, Dec. 2019. doi: 10.1109/JSYST.2018.2890062.

[29] Zhongkai Yi, Yinliang Xu, Jianguo Zhou, Wenchuan Wu, and Hongbin Sun. Bi-level programming for optimal operation of an active distribution network with multiple virtual power plants. *IEEE Trans. Sustain. Energy*, 11(4):2855–2869, Oct. 2020. doi: 10.1109/TSTE.2020.2980317.

[30] Chunyu Zhang, Qi Wang, Jianhui Wang, Pierre Pinson, and Jacob Østergaard. Real-time trading strategies of proactive DISCO with heterogeneous DG owners. *IEEE Trans. Smart Grid*, 9(3):1688–1697, May 2018. doi: 10.1109/TSG.2016.2597263.

[31] M. S. Bazaraa. *Nonlinear programming*. New York, NY, USA: John Wiley & Sons, Inc., 2nd edition, 1993.

[32] J.M. Arroyo. Bilevel programming applied to power system vulnerability analysis under multiple contingencies. *IET Gener. Transm. Distrib.*, 4(2):178–190, Feb. 2010. ISSN 1751-8687.

[33] Gurobi Optimization, LLC. Gurobi Optimizer Reference Manual, Dec. 2022. URL https://www.gurobi.com.

[34] ARKI Consulting & Development A/S. CONOPT. http://www.conopt.com, 2019.

[35] R. Fourer, D.M. Gay, and B.W. Kernighan. *AMPL: A Modeling Language for Mathematical Programming*. Duxbury, MA, USA: Thomson, 2nd. edition, 2003. ISBN 9780534388096.

[36] NASA Langley Research Center (LaRC). NASA POWER| Prediction of Worldwide Energy Resource. https://power.larc.nasa.gov/data-access-viewer/, 2023.

[37] N. Growe-Kuska, H. Heitsch, and W. Romisch. Scenario reduction and scenario tree construction for power management problems. In *Proc. IEEE Power Tech Conf.*, pages 1–7, Jun. 2003. doi: 10.1109/PTC.2003.1304379.